Water Science & Technology

IWA PUBLISHING

Water Science & Technology Vol 91 No 6, 757 doi: 10.2166/wst.2025.039

Modelling the effect of sediment and solid waste deposition on pluvial flood risk using *in situ* high-resolution rainfall and water level measurements

Hjalmar Olsson[a], Seith N. Mugume[b,*] and Johanna Sörensen[a]

[a] Department of Water Resources Engineering, Lund University, PO Box 118, Lund, Sweden
[b] Department of Civil and Environmental Engineering, Makerere University, PO Box 7062, Kampala, Uganda
*Corresponding author. E-mail: seith.mugume@mak.ac.ug

SNM, 0000-0002-8289-0099; JS, 0000-0002-2312-4917

ABSTRACT

Pluvial flooding is a significant threat in many Sub-Saharan African cities, driven by rapid urbanisation, climate change, failures, and insufficient hydraulic capacity of existing urban drainage systems (UDSs). However, limited modelling studies have investigated the effect of sediment and solid waste accumulation on the performance of UDSs during extreme loading conditions. In this research, the influence of combined scenarios of sediment and solid waste deposition and extreme rainfall on urban flooding in the upper Lubigi catchment in Kampala was investigated. The collected high-resolution rainfall data and water level observations in combination with field observations were used for model calibration and validation. The results show three locations that account for over 50% of the flooded volume in the catchment, based on the existing conditions. A near-complete blockage of sediment and solid waste at three culvert crossings increased the flood volumes by up to 40% for higher ($\geq$50 years) return periods and by up to 105% for low return periods ($\leq$10 years). This research underscores the importance of using high-resolution rainfall data in flood modelling, as well as the necessity of improved UDS asset management, and effective solid waste and sediment management in order to achieve resilient and sustainable water management in cities.

Key words: 1D hydraulic modelling, high-temporal resolution rainfall measurements, pluvial flood risk, sediments, solid waste, water level measurements

HIGHLIGHTS

- Utilised high-resolution rainfall and water level measurements for model calibration and validation.
- Modelled scenarios combining extreme rainfall, sediments, and solid waste deposition.
- Identified three locations accounting for more than 50% of the flooded volume in the Lubigi upstream catchment.
- Approximately 105% increase in the total flood volume for rainfall with a 2-year return period due to increased sediment and solid waste.

GRAPHICAL ABSTRACT

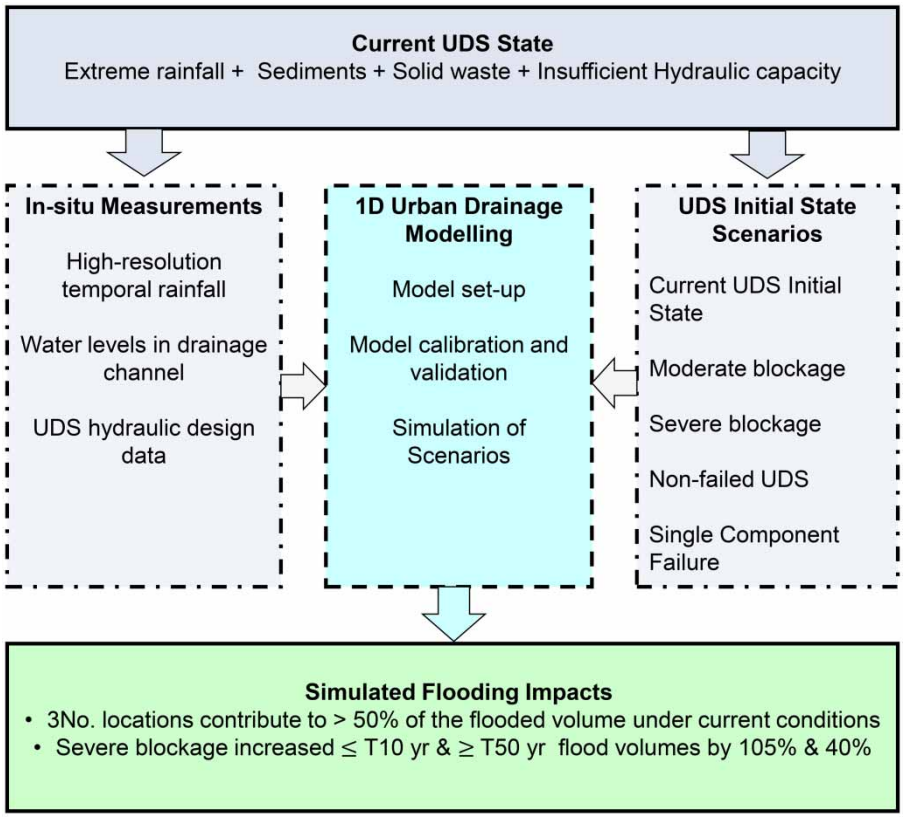

INTRODUCTION

Many rapidly urbanising Sub-Saharan African cities are grappling with increased risk of urban flooding caused by urban creep, peri-urban expansion, increasing dry weather flows, inadequate capacity of existing urban drainage systems (UDSs) and insufficient solid waste management practices (Owusu & Oteng-Ababio 2015; Sohn *et al.* 2020; OECD/UN/ECA/AfDB 2022; IPCC 2023; Møller-Jensen *et al.* 2023; MacAfee & Löhr 2024; Mugume *et al.* 2024b).

Furthermore, it has been projected in recent studies that climate change will exacerbate the risk of pluvial, fluvial, and coastal flooding in many parts of Africa due to increased frequency and intensity of extreme rainfall, rising sea and inland lake water levels, expansion of urban areas in low-lying flood-prone areas, and low adaptive capacity (Owusu & Oteng-Ababio 2015; Trisos *et al.* 2022; IPCC 2023; Møller-Jensen *et al.* 2023; Mugume *et al.* 2024a).

Urban pluvial flooding occurs when runoff caused by extreme rainfall exceeds the capacity of an existing UDS (Maksimović *et al.* 2009). In many developing countries, sediment and solid waste deposition in the existing UDSs can further reduce the hydraulic conveyance capacities, leading to increased risk of pluvial flooding (Barthelémy *et al.* 2016). In addition, uncontrolled discharge of untreated sewage into separate stormwater systems, sewer overflows, and cross-connections often lead to the pollution of receiving waters and the occurrence of water-borne diseases (Chen *et al.* 2022; Wu *et al.* 2024).

The conventional UDS design is focused on minimising the probability of occurrence of failures using pre-defined average recurrence intervals (Mugume & Butler 2017; Haghighatafshar *et al.* 2020). However, to enhance the resilience of UDSs, a risk-based paradigm shift that considers all possible failure scenarios is required (Mugume *et al.* 2015; Haghighatafshar *et al.* 2020).

Kampala, the capital of Uganda has experienced increasing frequency and magnitude of pluvial flooding events in recent years, particularly in low-lying and low-income areas, due to rapid urbanisation, sediment and solid waste accumulation, inadequate capacity of the existing UDSs and insufficient UDS asset management practices (Sliuzas *et al.* 2013; Mugume *et al.* 2015; Pérez-Molina *et al.* 2017; Richmond *et al.* 2018; Arinabo 2022; Adeke & Mugume 2025).

A number of recent modelling studies have been conducted to investigate the causes of flooding and quantify the resulting impacts in Kampala. Kiyengo *et al.* (2019) applied geographic information system (GIS)-based spatial analysis and two-dimensional (2D) modelling using the Hydrologic Engineering Center's River Analysis Software (HEC–RAS) to assess the spatial and temporal flooding patterns in Kampala's Lubigi catchment, considering data spanning the period from 1983 to 2014. The study findings suggested that extreme floods occurred once every 3 years during the study period.

Habonimana (2014) used high-resolution rainfall data to calibrate a Weather Research and Forecasting model and applied the data to develop a flood model for the Lubigi upper catchment. The study findings suggested that high-intensity, short-duration rainfall results in more severe flooding impacts when compared to long-duration, low-intensity rainfall events.

In another study, Pérez-Molina *et al.* (2017) developed a cellular automata model to simulate the effect of urban growth on flooding in the upper Lubigi catchment. The findings suggested that due to rapid urbanisation, policies focused on the preservation of urban wetlands are insufficient in minimising the projected urban flooding impacts, thus necessitating the implementation of combinations of flood reduction strategies.

In a recent study, Mugume *et al.* (2024b) developed a coupled 1D–2D model to evaluate the effectiveness of blue-green infrastructure (BGI) on flooding considering scenario combinations of 'failed' and 'non-failed' UDS initial states and extreme rainfall. The study results suggested that catchment-scale implementation of multifunctional rainwater harvesting systems could lead to a reduction in the total flood volume of 16–45% and contribute to the enhancement of existing UDS resilience to flooding.

However, most of the studies were undertaken using the historical daily rainfall data for Kampala, which was disaggregated using the TRRL East African Flood Model (Fiddes *et al.* 1974). Furthermore, there are limited studies that have investigated the effect of sediment deposition and solid waste deposition on pluvial flooding in East African cities.

Min & Tashiro (2024) developed a coupled 1D–2D model using an InfoWorks ICM model in Yangon, Myanmar, utilising high-temporal resolution rainfall data and measured water level data from loggers as model inputs. The study findings suggested that sediment and solid waste deposition and receiving water level variations, such as tidal effects, contribute more to pluvial flooding when compared to extreme rainfall. In a similar study, Pervin *et al.* (2020) modelled the effect of solid waste on flood risk using case studies of UDSs in Sylhet, Bangladesh, and Bharatpur, Nepal using calibrated and validated hydraulic models. The study results suggested that solid waste deposition contributed to 18.5 and 7.6% increase in flood risk in Sylhet and Bharatpur, respectively. Finally, a similar study by Quang *et al.* (2022) developed and applied a numerical model to investigate the effect of sediment deposition on urban drainage performance. The study findings suggested that a 40% reduction of the conduit cross-section area resulted in lower reduction (60–70%) of the hydraulic performance of the conduit when compared to a corresponding increase in Manning's roughness coefficient which led to 80–90% reduction in the hydraulic performance of the conduit.

Based on the critical review of recent studies, there exists a critical need to undertake research focused on modeling the effect of sediment and solid waste deposition on pluvial flooding in cities. This is largely attributed to the complex interplay of urbanization that leads to abrupt changes in urban form, increased frequency of occurrence of extreme rainfall, inadequate hydraulic capacity of the existing UDSs, and sediment and solid waste accumulation, which in combination lead to more severe urban flooding impacts. It is, therefore, crucial to investigate these dynamics in order to develop appropriate strategies for enhancing flood resilience in cities. In this respect, therefore, the main objective of this study is to investigate the effect of sediment and solid waste deposition in UDSs on urban flooding. More specifically, this study aims to identify locations vulnerable to flooding in the Lubigi catchment, considering scenarios of combinations of sediment and solid waste deposition rates and extreme rainfall. The following research questions formed the basis for the study:

- Can *in situ* high-resolution rainfall and water level measurements facilitate accurate modelling of flooding impacts in failed UDSs?
- How do variations in the rates of sediment and solid waste deposition and the occurrence of extreme rainfall influence flooding in the existing Lubigi UDS?

To address the aforementioned research questions, a new methodology was developed, combining a collection of *in situ* high-resolution rainfall and water level measurements with 1D hydraulic modelling of scenarios that combine extreme rainfall, sediment, and solid waste deposition rates to quantify the resulting flooding impacts in the existing Lubigi UDS in Kampala. The findings of this study underscore the critical importance of consideration of sediment and waste deposition for more accurate modelling of pluvial flooding impacts in developing cities.

PROPOSED APPROACH AND METHODOLOGY

This study investigated the hydraulic impacts of sediment and solid waste deposition during varied flow conditions. In combination with sediment and solid waste deposition, different rainfall events were modelled based on the recently observed high-resolution rainfall data and recorded historical rainfall (IDF curves) with a fixed duration of 30 h and varied return periods of 2, 10, 50, and 100 years. A 1D hydraulic model was built in PCSWMM, based on the drawings from Kampala Capital City Authority (KCCA), digital elevation maps (DEMs), and field visit findings. To calibrate and validate the model, a tipping bucket rain gauge was installed to collect high-resolution rain data, and water level observations were conducted in the Lubigi primary channel. Additionally, several field observations were made to verify the technical drawings of the existing UDS. An overview of the proposed approach and methodology is shown in (Figure 1), with a more detailed description provided in the following sections.

1D modelling approach

PCSWMM, developed by Computational Hydraulics Inc, was used to create the 1D model. PCSWMM is a widely used modelling program for urban drainage and flooding studies all over the world (Chitwatkulsiri *et al.* 2022; Ortega Sandoval *et al.* 2023; Mugume *et al.* 2024b). PCSWMM uses the United States Environmental Protection Agency (US EPA) EPA SWMM5.2 dynamic rainfall–runoff simulation engine (Rossman & Simon 2022) along with support tools like GIS technology. PCSWMM offers the option to choose from different methods for flow routing. Dynamic wave routing is the most comprehensive routing method, involving computation of the full Saint-Venant flow equations (Rossman & Simon 2022). This approach can represent pressurised flow, with flooding occurring when the water depth at a node surpasses the maximum available depth. The flooded volume is either lost from the system or ponded atop of the node. The ponded volume on top of the node is, subsequently, allowed to re-enter the system when hydraulic capacity is available. The dynamic wave routing approach can account for backwater effects, flow reversal, and local head losses (Rossman & Simon 2022).

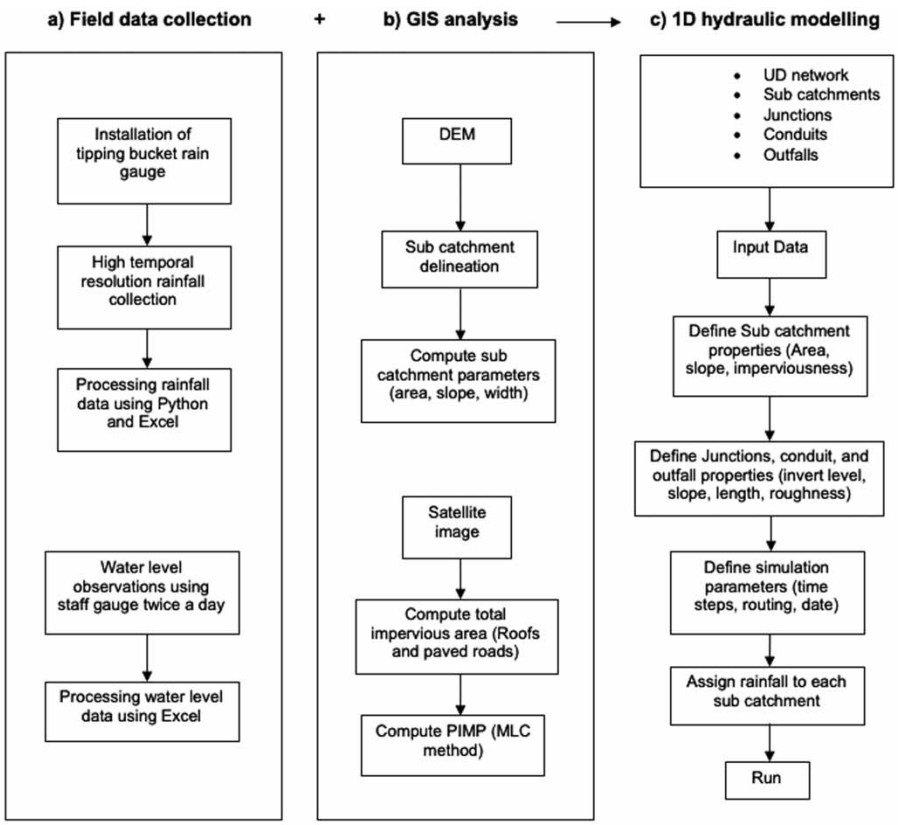

Figure 1 | Adopted study approach for field data collection, GIS analysis, and 1D hydraulic modelling.

In this study, dynamic wave routing was used without allowing ponding, meaning that when a node floods, the flooded volume is lost from the system. In PCSWMM, Saint-Venant's equations for continuity (Equation (1)) and momentum (Equation (2)) are used to describe the unsteady flow routing in closed and open conduits. Both equations are solved initially using an explicit finite difference estimate to solve the derivatives in Equations (1) and (2), followed by an iterative refinement process to ensure stability and convergence (Butler *et al.* 2024). To achieve numerical stability in the model, small time steps of 30 s or less are needed when using Dynamic wave routing (Rossman & Simon 2022).

$$B\frac{\partial y}{\partial t}+\frac{\partial Q}{\partial x}=0, \tag{1}$$

$$\frac{\partial Q}{\partial t}+\frac{\partial}{\partial x}\left(\frac{Q^2}{A}\right)+gA\frac{\partial y}{\partial x}-gA(S_o-S_f)=0, \tag{2}$$

where B is the width; y the depth; t the time; Q the flow; x the distance; A the cross-sectional area of flow; S_o the bed slope; and S_f the friction slope.

Rainfall observations

Kampala has two major rain seasons occurring from March to May and from September to November and receives an average annual rainfall of 1,292 mm (Mugume 2015; Nimusiima *et al.* 2021). April is, in general, the wettest month, with approximately 180 mm of average monthly rainfall, while July is the driest month, receiving around 60 mm of the average monthly rainfall (Mugume 2015).

In this research, a HOBO Data logging Rain Gauge RG3-M (tipping bucket rain gauge) was installed within the grounds of the Lubigi wastewater treatment plant located at latitude 0.3474310 and longitude 32.5487220 on 28th February 2024, to obtain high-resolution rainfall data (Figure 2). The location at the Lubigi faecal sludge and wastewater treatment plant

Figure 2 | Installed tipping bucket rain gauge mounted 50 cm above ground.

was selected to minimize unwanted interference with the device. To avoid splashing and puddles, the rain gauge was mounted 50 cm above ground on top of a wooden construction. The rain gauge was calibrated following the HOBO Data Logging Rain Gauge RG3-M manual (Olsson 2024). In this study, observations from 1st March to 30th April 2024, were used. Data preparation and cleaning was undertaken on the rainfall dataset to ensure that the correct format was entered in PCSWMM. In addition, the data were transformed from seconds to 5-min time steps, which reduces the data size while maintaining high-resolution temporal resolution.

Water level observations

A water level gauge was used for observing water level variations (Figure 3). The water level gauge installed by the Ugandan Ministry of Water and Environment is located at the Hoima Road box culvert crossing with location coordinates of 0.347107, 32.541358 (longitude and latitude), which is 825 m downstream of the rain gauge location. Two water level measurements were taken on a daily basis, i.e. in the morning and the afternoon. In addition, on days when it rained, an extra measurement was taken immediately after the occurrence of the rainfall event to capture the peak water levels at the outfall. If the rainfall event occurred during the night, the peak level was measured, as indicated by debris and maximum water level marks on box culvert walls. In this study, the water level observations covered the same period as the collected high-resolution rainfall data.

Case study 1D-model setup

Kampala is characterised by steep hills and a densely built urban environment. A case study was conducted in a 33 km^2 area in the upstream part of the 64 km^2 Lubigi catchment (Figure 4), reaching from 1,161 to 1,309 m above the mean sea level. The upstream part consists mainly of urbanised areas, one primary channel, and eight secondary channels. In the downstream part of the upper catchment, water flows through the Lubigi wetland, which is one of the largest wetlands in Kampala (KCCA 2016). Before the wetland, water flows close to the Lubigi wastewater treatment plant, where the rain gauge is located.

Figure 3 | Water level staff gauge located in the primary Lubigi channel at the Hoima Road box culvert crossing.

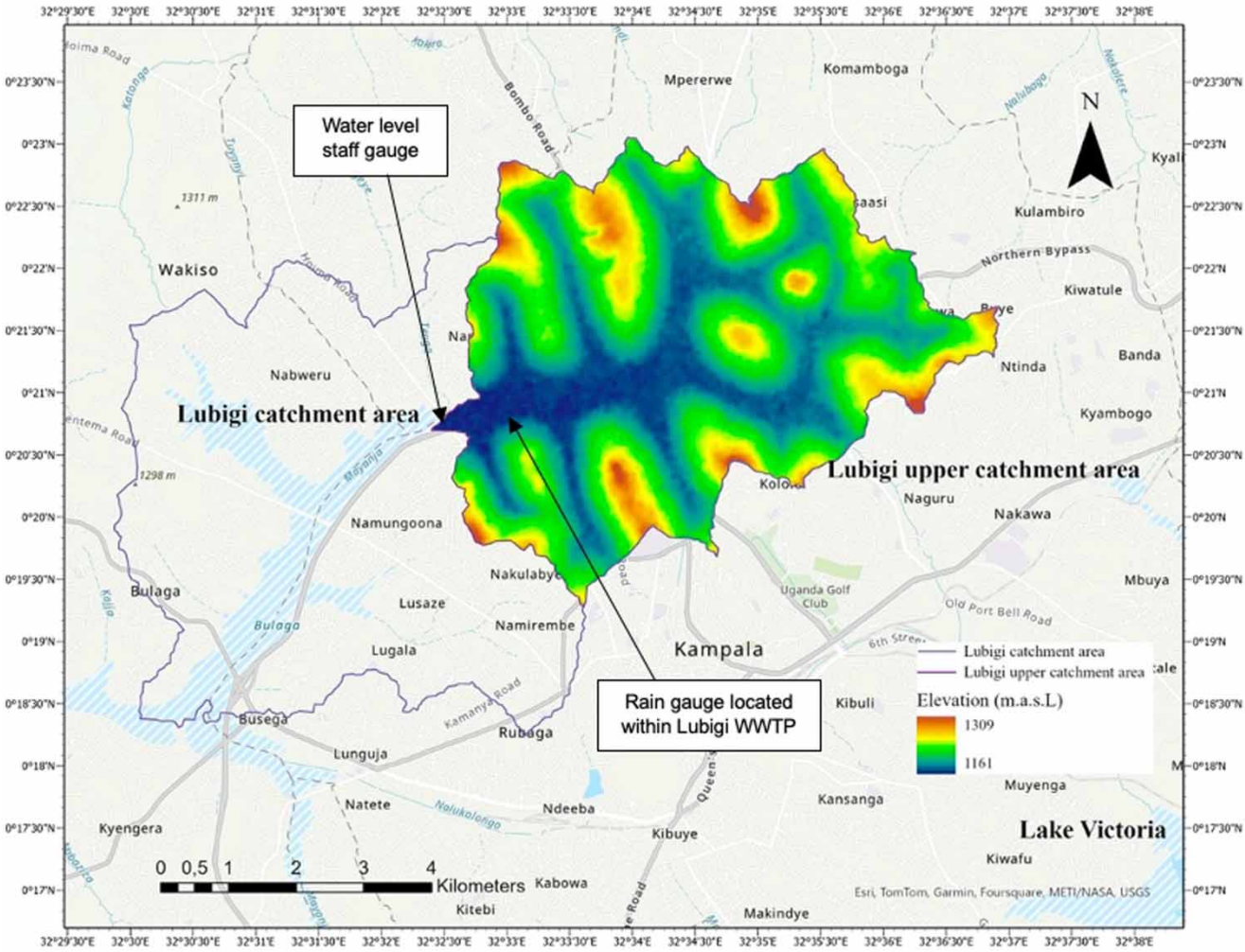

Figure 4 | Lubigi catchment with the upstream part of the Lubigi catchment, which is included in the model, shown with elevations from the DEM.

The model of the existing UDS that drains the upstream Lubigi catchment was built as a 1D hydraulic model in PCSWMM. The primary and secondary channels consist mainly of open trapezoidal channels of concrete, stone pitching, and earth material. The open channels connect with concrete box culverts and pipe culverts located at the existing road crossings. In 2020–2021, the primary channel from Gulu Highway at Bwaise to Hoima Road and the secondary Nakamiro channel were relined using cable concrete lining (KCCA 2020). The 1D-model setup was applied using the case study specific data described in Table 1.

GIS-based spatial analysis was undertaken using ArcGIS software to delineate the catchment into sub-catchments and to calculate sub-catchment areas, percentage slopes, and widths. Additionally, surface types were calculated from spectral imagery using ArcGIS spatial analysis. Roofs and paved roads were assumed to be impervious, while the remaining surface types were considered pervious. The percentage of impervious surfaces was calculated to be 74% for the whole catchment area (Figure 5). Since this is a large urbanised catchment with an area of 33 km^2, the same percentage of imperviousness (PIMP) was considered for all sub-catchments to minimise computational complexity entailed in the determination of the percentage of imperviousness for the individual sub-catchments. Such an approach, despite having inherent uncertainty due to the averaging of the percentage of imperviousness, has been applied successfully to minimise the computational resources required to undertake coupled 1D–2D surface flood modelling for the Kinawataka and Nalukolongo catchments in Kampala City (Mugume *et al.* 2024b).

Table 1 | Information on data used in the 1D model

Data set	Quality and resolution	Data period or date of publication	Source	Purpose
Tipping bucket rain gauge	High-resolution rainfall (mm)	1st March–30th April 2024	Primary source	Model calibration and extreme rainfall analysis
Staff water level gauge	Water level (m)	1st March–April 2024	Primary source	Model calibration and validation
77-year daily rainfall for Makerere University rain gauge station	Daily rainfall (mm)	1943–2019	Uganda National Meteorological database	Extreme rainfall analysis
Shuttle Radar Topography Mission (SRTM) Digital Elevation Model	30 m × 30 m spatial resolution	23-September-2014	USGS SRTM	Digital elevation data for dividing into catchment and sub-catchments
Sentinel-2 satellite image	5 m × 5 m spatial resolution	22-August-2023	Copernicus	Land-use and land cover analysis imperviousness (PIMP) from spectral imagery in ArcGIS
Base map World Imagery ArcGIS Pro	0.31 m (1), 0.46 m (2), 0.31 m (3) spatial resolution	15-October-2022 (1), 20-February-2023 (2), 16-April-2023 (3)	Esri, ArcGIS Pro	Land-use and land cover analysis imperviousness (PIMP) from spectral imagery in ArcGIS
Existing and designed urban drainage network data (open channels, cross culverts)	UDS parameters (bottom width, side slopes), lengths of channel sections, invert levels, slopes, cross culvert diameters	2016 and 2020	KCCA reports and design drawings	Channel morphology for the 1D urban drainage model

Hydraulic data for the primary and secondary channels was obtained from KCCA (2016). The data used included open channel cross-section dimensions (depth, bottom widths, and side slopes), material, and length. In addition, information on culvert crossings, including cross-sectional dimensions (height and widths), type of culvert, number of barrels, material, and length, was used. For the relined primary channel and the secondary Nakamiro channel, design maps were obtained from KCCA (2020), which included more detailed drawings than KCCA (2016), as well as invert levels. Unfortunately, as-built maps were not available. The invert levels in KCCA (2020) served as a basis for calculating the invert levels for the rest of the catchment area using the given slopes and open channel lengths from KCCA (2016). In addition, site visits were conducted to verify the data obtained from KCCA (2016). Data for open channel and culvert dimensions, material, and culvert type were corrected for some sections after the site visits.

In the developed model, upper Lubigi UDS comprises 35 sub-catchments (green in Figure 6), 348 conduits, 346 junctions, and drains into Lubigi wetland. All sub-catchments were assigned to the same rain gauge (Figure 6). To avoid placing the outfall in the model close to the observation point and to account for water downstream that impacts the upstream catchment area, the primary channel was extended until the Sentema Road crossing, including parts of the Lubigi wetland located downstream of the observation point. This extension included 10 supplementary sub-catchments (Figure 6, blue), 9 conduits, 8 junctions, and 2 outfalls downstream of the studied catchment. The primary channel in the wetland has a notably smaller cross-section compared to the primary channel upstream of the wetland. Note that there are no secondary channels transporting water between sub-catchments in the added, downstream area (Figure 6, blue). However, such channels do exist but were not included in this analysis. In the wetland, the cross-sectional area and the invert level of the primary channel, located 100 m downstream of Hoima crossing, were measured in the field. The same cross-section and slope for the primary channel in the wetland have been assumed until the outfall. Field observations indicated that most of the base flow, originating from shallow groundwater and wastewater, flows through the primary channel. However, at high flows, the primary channel is unable to convey all the water, causing water to flood into the existing wetland. To model this, a second, parallel conduit was added, connecting to the Hoima Road crossing at 0.5 m above the invert level. This second conduit was designed as a

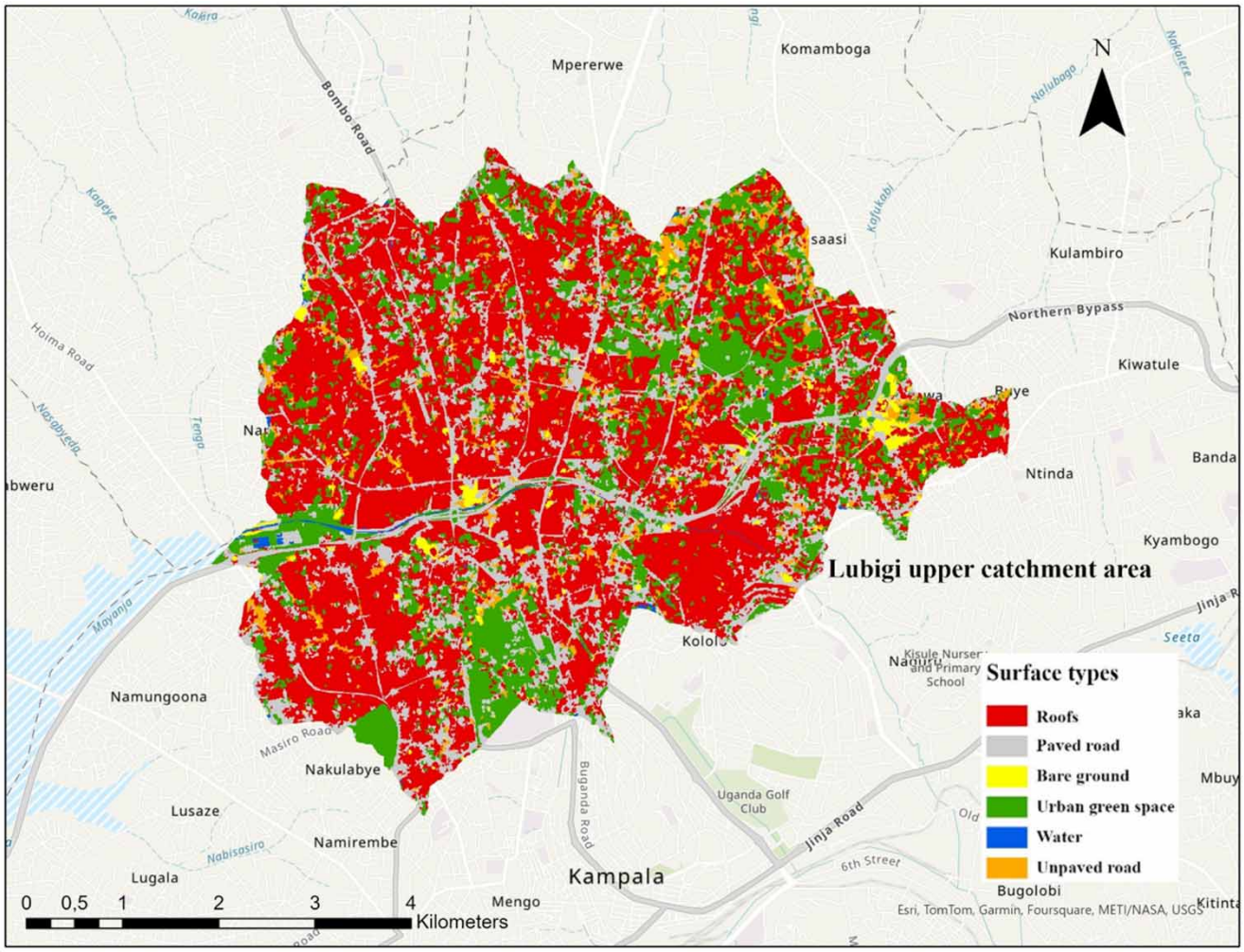

Figure 5 | Surface types analysed from spectral imagery using ArcGIS spatial analysis.

wide, open channel with a seepage rate and an outfall. It was dimensioned using the data from KCCA (2016), containing cross-sectional data (depth, bottom widths, and side slopes). This setup allows water to flow via the primary channel at the base flow, while at higher flows, water is also converted to the second conduit to mimic the wetland flow.

Extreme rainfall analysis

The two largest rainfall events recorded by the installed tipping bucket rain gauge are shown in Figure 7. Both rainfalls have early peaks: rainfall *RE1* that occurred on 6th March 2024, peaked at $t = 10$ min, while rainfall *RE2* that occurred on 23rd April 2024, peaked at $t = 25$ min. However, *RE1* has a more distributed volume, whereas most of the rainfall in *RE2* occurs at the beginning of the event.

Furthermore, the intensity–duration–frequency (IDF) curves derived for the Lubigi upstream catchment are shown in Figure 8. The IDF curves were derived using the annual maximum series method using observed 77-year daily rainfall between 1943 and 2019 for Kampala (Mugume *et al.* 2024b). To incorporate the effects of the current climate change, Mugume & Nakyanzi (2024) suggest a climate change factor of 1.24–1.44 for Kampala. Therefore, a climate change factor of 1.3 was applied to upscale the 77-year daily rainfall dataset. When comparing historical rainfall data with the recorded rainfall in Figure 8, the average intensity of the recorded rainfall events is approximately 25% lower than that of a 2-year return period event.

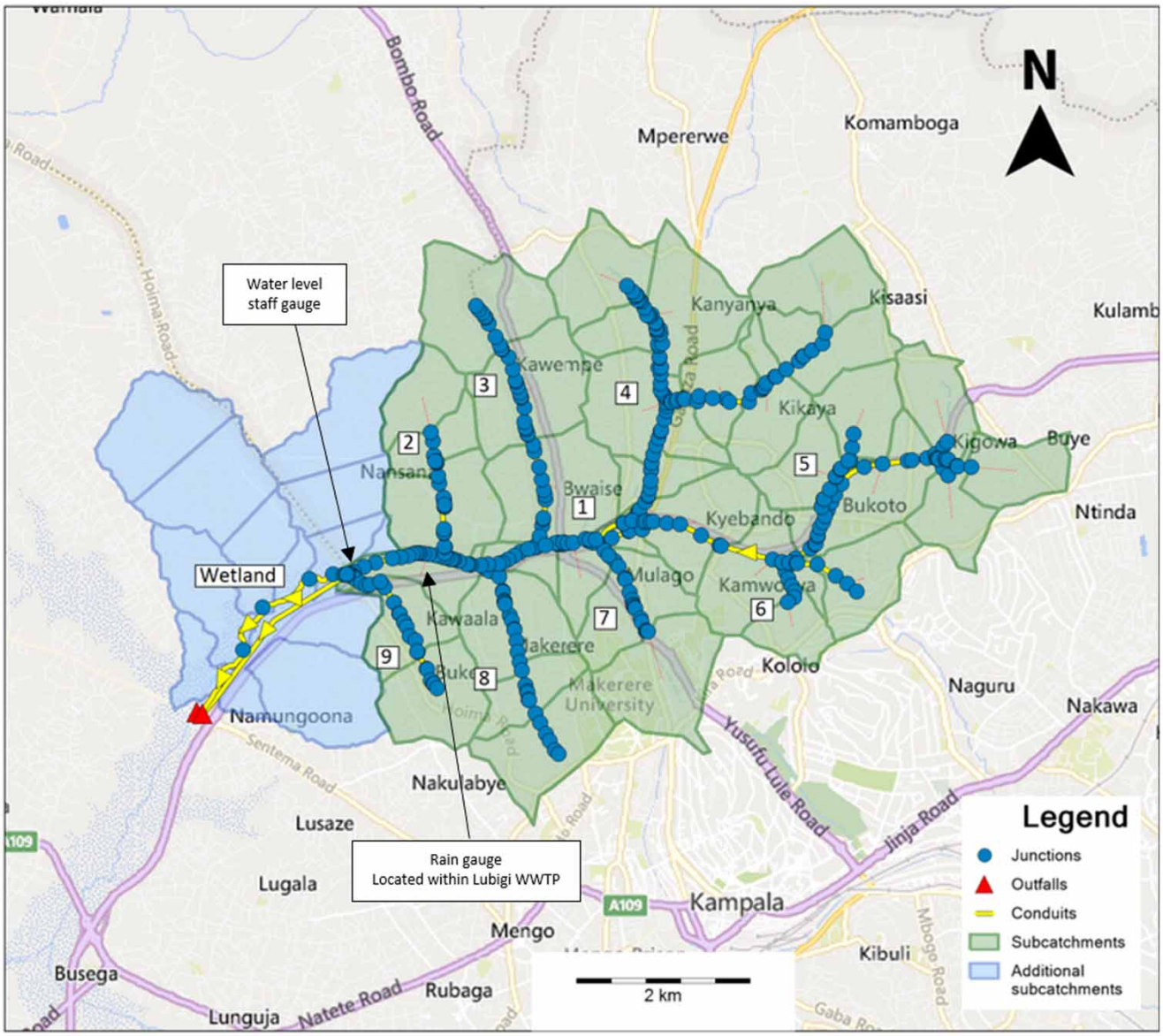

Figure 6 | Overview of the modelling setup in PCSWMM showing the primary open channel (1) and eight secondary channels (2–9). The catchment area (green) is delineated into 35 sub-catchments and extended with eight more additional sub-catchments (blue) to account for water downstream that could affect the upstream catchment area.

To account for the larger rainfall events in the model, design storms were created using the alternating block method (Chow *et al.* 1988; Balbastre-Soldevila *et al.* 2019) In the alternating block method, the design hyetograph produced specifies the rainfall depth occurring in n successive time intervals of duration Δt over a total duration $T_d = n\Delta t$. After selecting the design return period, the rainfall intensity is read from the IDF curve for each duration and the corresponding rainfall depth computed as a product of intensity and duration. Thereafter, the amount of rainfall to be added for each additional time step (block) is computed as the difference between successive rainfall depths. Subsequently, the blocks are reordered in a time sequence, centring the maximum intensity at the required duration T_d, and arranging the rest alternately on either side of the central block (Chow *et al.* 1988).

During the derivation of the design storms, an areal reduction factor (ARF) of 0.885, based on the catchment area of 33 km^2, was applied to account for the difference between point rainfall and areal rainfall. The ARF was computed using the transport and road research laboratory (TRRL) East African flood model, an approach for the prediction of design

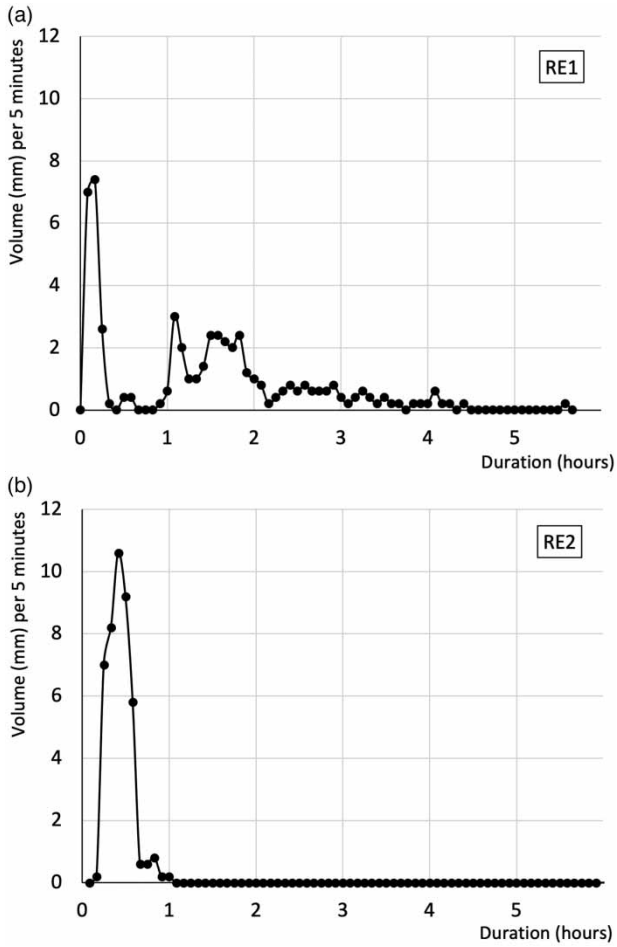

Figure 7 | Largest recorded rainfalls during the period 1st March to 30th April, 2024. (a) *RE1* with a total volume of 52.6 mm and (b) *RE2* with a total volume of 43.4 mm. Each point represents the volume grouped into 5-min intervals.

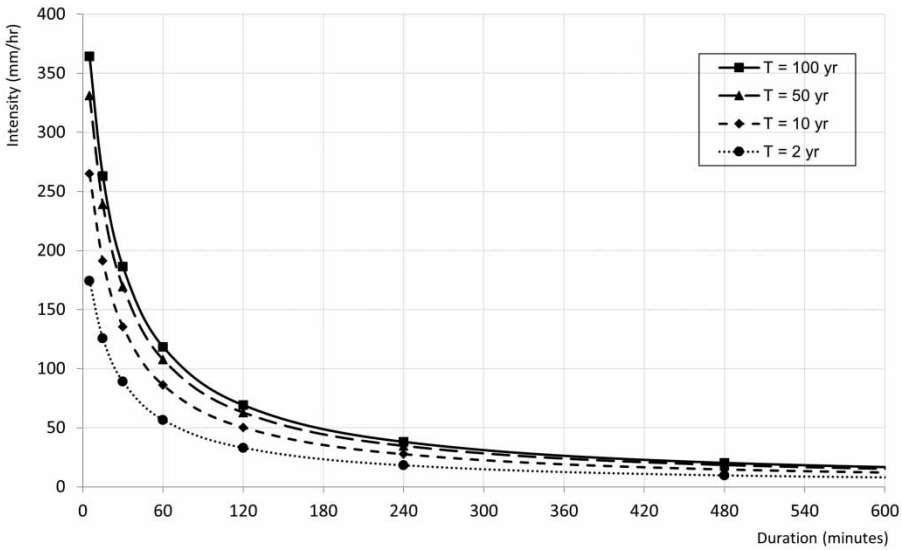

Figure 8 | IDF curves for the Lubigi upstream catchment using a change factor of 1.3 to account for the current climate change.

storm characteristics in East Africa (Equation (3)) that was based on an extensive rainfall dataset obtained from 867 rain gauge stations and spanning a period of 40 years, from 1926 to 1968 (Fiddes *et al.* 1974; MoWT 2010).

$$\mathrm{ARF} = 1 - 0.044A^{0.275}, \tag{3}$$

where ARF is the areal reduction factor and A is the area of the catchment.

A similar approach is described in the widely adopted *Wallingford Procedure*, which is based on a comparison of point and areal rainfall data for areas where several rain gauges exist (Butler *et al.* 2024).

Four design storms were created for return periods, T of 2, 10, 50, and 100 years, and with a duration of 30 h (Figure 9). The 30-h design storms were utilised in this study, despite the relatively short computed time of concentration and duration of the measured rainfall events, to ensure that the developed model adequately captures the effect of antecedent soil moisture conditions, progressive saturation of the soil system, and achieves steady-state conditions to facilitate more accurate simulation of the peak flows at the outfall (Krvavica & Rubinić 2020).

Sensitivity analysis and calibration

A one-at-a-time sensitivity analysis was conducted to identify the most sensitive model parameters. A total of 15 parameters in PCSWMM were included. The parameters were changed one at a time by increasing and decreasing its value by 50% while the rest of the parameters remained unchanged. *Manning's roughness coefficient for channel flow*, *average value baseflow*, and *percentage imperviousness* were determined to be the most sensitive parameters. As described above, the percentage imperviousness had been calculated by using ArcGIS spatial analysis of spectral imagery; therefore, this value remained unchanged and Manning's roughness coefficient for channel flow and average value base flow were adjusted during calibration.

The model was calibrated using two recently observed high-resolution temporal rainfalls from March: rain event *RE1* (shown in Figure 7) and a rain event of 13.4 mm on 27th March, along with the corresponding observed water levels at

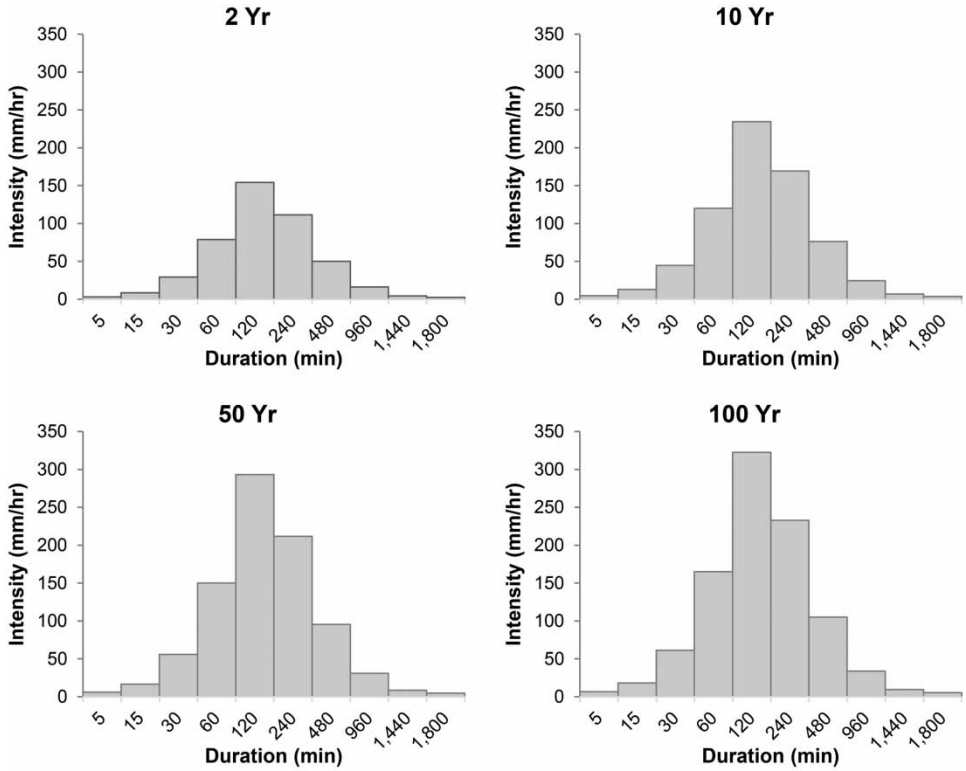

Figure 9 | Design storms for the Lubigi catchment area for four return periods (*T2*, *T10*, *T50*, and *T100* years) and a fixed duration of 30 h. The rainfall peak occurs at $t = 120$ min.

the Hoima box culvert crossing. The calibration entailed manual adjustment of Manning's n value for channel flow and average base flow to match the observed water level peaks before and after rainfall, while ensuring that the model parameters remained within reasonable bounds.

Because of calibration, the primary and secondary channels containing sediment and solid waste, and the wetland were assigned a Manning's roughness coefficient of 0.05. Secondary channels without sediment and solid waste were assigned a Manning's roughness coefficient of 0.0200–0.0325 depending on their specific characteristics. Culvert crossings currently containing sediment and solid waste were assigned a Manning's roughness coefficient of 0.10. The primary and secondary channels were assigned average base flows of 4 dm^3/s and 1 dm^3/s, respectively.

Validation

The model was validated using rainfall and water level observations ranging from 5th April to 23rd April 2024. A total of 40 water level observations, covering 11 rainfall events, were included. The validation was evaluated with the Nash–Sutcliffe efficiency (NSE) and the root mean square error (RMSE) (Equations 4 and 5).

NSE is a goodness-of-fit indicator that is calculated by subtracting the ratio of the mean square error between the observed and modelled values (Ritter & Muñoz-Carpena 2013) (Equation 4):

$$\mathrm{NSE} = 1 - \frac{\sum_{i=1}^{N} (O_i - P_i)^2}{\sum_{i=1}^{N} (O_i - \bar{O})^2}, \tag{4}$$

where O_i represent the observed values, P_i represent the modelled values, and $\bar{O}$ is the mean of the observed values. An NSE of $= 1$ indicates a perfect fit while an NSE ≤ 0 indicates that the mean observed values serve as a more accurate indicator than the model.

RMSE indicates the prediction error in a model (Ritter & Muñoz-Carpena 2013) (Equation 5).

$$\mathrm{RMSE} = \sqrt{\frac{\sum_{I=1}^{N} (O_i - P_i)^2}{N}}, \tag{5}$$

where O_i represents the observed value and P_i represents the modelled value. A RMSE $= 0$ indicates an ideal fit.

Experiment design and scenario description

Simulation of various scenarios of sediment and solid waste deposition was carried out by adjusting Manning's roughness coefficient for conduits (for all scenarios) and by reducing the cross-sectional areas of culvert crossings at three locations: Kawaala, Nakamiro, and Bombo road crossing (for Scenarios 2 and 3, Figure 10). While observations in the field showed that sediment and solid waste also accumulated in the open channels, accumulation was more evident in the culvert crossings, leading to blockages and backwater effects. This led to the decision to simplify the failure modelling approach by varying the cross-sectional area of the culvert crossings only. To investigate the effect of changes in hydraulic loading resulting from various rainfall scenarios, the largest recorded rainfall and four extreme rainfalls of 2-, 10-, 50- and 100-year recurrence were simulated in combination with the following sediment and solid waste deposition scenarios:

Scenario 1: *Current sediment and solid waste deposition*: The existing UDS under the current conditions of sediment and solid waste deposition. These conditions were calibrated and validated.

Scenario 2: *Moderate blockage*: Culvert cross-sectional area reduced by 50% at Kawaala, Nakamiro, and Bombo Road crossings, reflecting significant, but not complete blockages.

Scenario 3: *Severe blockage*: Culvert cross-sectional area reduced by 80% at the Kawaala, Nakamiro, and Bombo Road crossings, representing a near-complete blockage.

Scenario 4: '*Non-failed' UDS*: Manning's roughness coefficient of all the links in the modelled UDS is set to a uniform value of 0.020, representing the desired UDS initial state condition, in which all the system components are well maintained and clean.

Figure 10 | Culvert crossings with increased sediment and solid waste blockage, used for Scenarios 2 and 3. The numbers next to the channels are the same as in the overview, shown in Figure 6. Kawaala and Bombo Road crossings are located on the primary channel (1), and Nakamiro crossing is located on a secondary channel (3).

Scenario 5: *Single component failure*: Manning's roughness coefficient of every single component (culvert crossing) was increased to 100, representing the complete failure of the culvert crossing.

RESULTS

Model performance

The validation was executed for 40 water level observations from April 2024. The NSE resulted in 0.81, which was considered acceptable. The RMSE was calculated to be 0.18 m, compared to the standard deviation, which was 0.41 m.

In Figure 11, the modeled water levels are plotted against the observed water level to visualize the validation and calibration results. The reference line is used to see model accuracy. A value above the line means that the model overestimates the water level, and vice versa. A value on the reference line means a perfect fit.

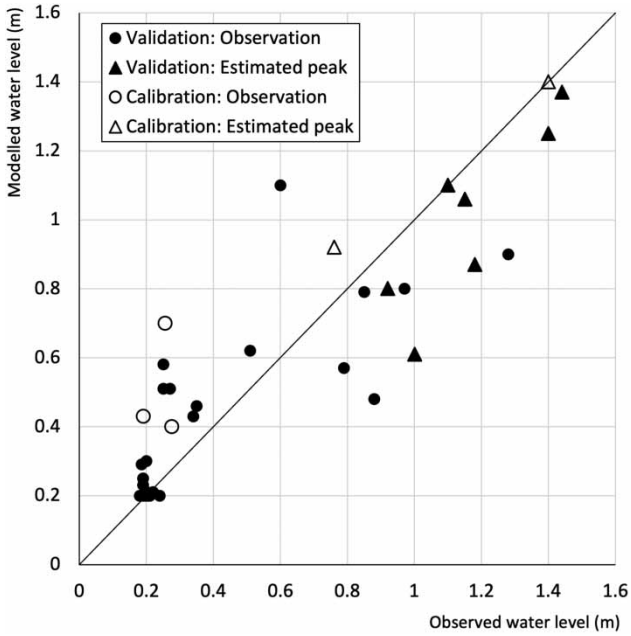

Figure 11 | Calibration and validation results. The modelled water level is plotted against the observed water level. The circular symbols represent a measured water level at a specific time, while the triangular symbols represent an estimated peak water level based on the observed high-level flood marks on the Hoima Road box culvert wall.

Locations vulnerable to flooding

By running the model with a time series of the recent observed rainfalls and current sediment and solid waste deposition, three locations vulnerable to flooding were identified: Bwaise, Alice Kaggwa Road, and Kamwokya Kisalosalo Road (Figure 12).

Table 2 shows the flooding loss at these three locations. In the model, flooding loss refers to water that has overflowed the drainage system and is no longer part of the drainage network. This could be described as flooded water being spread out on the surface, effectively being 'lost' from the drainage system and not returning to the source. For the recorded rain event *RE1*, described in Figure 7, flooding at Bwaise, Alice Kaggwa, and Kamwokya Kisalosalo accounted for 57% of the total flooding in the catchment. For the synthetic *T10* and *T100* rain events, flooding was approximately 20% compared to the entire catchment area. It should be noted that the recorded rain event *RE1* was 52.6 mm over 5.5 h, while the synthetic *T10* and *T100* rain events were 113.7 and 156 mm, respectively, both over 30 h.

Scenario analysis

The following section presents the results from the scenario analysis, summarised in Table 3. Scenario 3 resulted in a large percentage increase in the total flood volume when compared to Scenarios 1 and 2, particularly for the rainfall events with lower return periods (*RE1* and *T2*). In addition, Scenarios 2 and 3 led to an increase in upstream flooding when compared to Scenario 1, which was attributed to backwater effects caused by increased sediment and waste deposition in downstream sections of the existing Lubigi UDS.

The study results suggest that flooding increases with higher rainfall return periods, sediment, and solid waste deposition. The computed flooding loss to rainfall runoff ratio also increased with the increasing rates of sediment and solid waste deposition. Furthermore, the observed rain event *RE1* resulted in a higher flooding loss ratio when compared to design storm *T2* and was comparable to the corresponding Scenario 3, *T10* results. In addition, the study results indicated that low return period rainfall events (*RE1* and *T2*) led to a high increase in the total flood volume.

The study results obtained in Scenario 4 show that enhancing UDS cleaning and maintenance can contribute to the significant reduction of the resulting flooding impacts between 23 and 57% when compared to the corresponding results obtained in Scenario 1. However, the Scenario 4 study results also suggest that even if the existing UDS is cleaned and well maintained, residual flooding is caused by the occurrence of extreme rainfall events with return periods, $T \geq 10$ years (Figure 13).

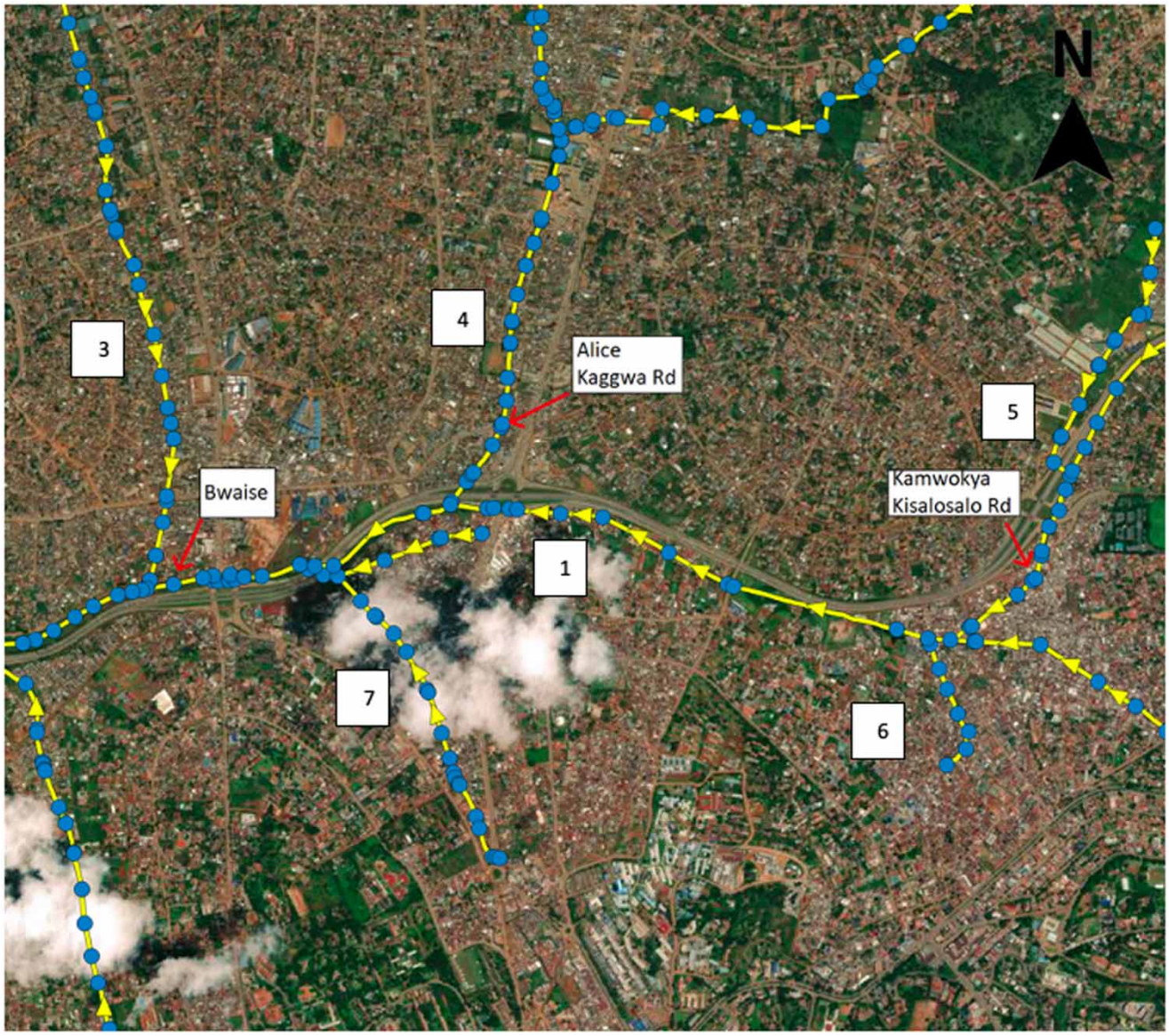

Figure 12 | Locations vulnerable to flooding. The numbers next to the channels are the same as in the overview, shown in Figure 6.

Table 2 | Flooding losses at Bwaise, Alice Kaggwa Road, and Kamwokya Kisalosalo Road

Rainfall	Bwaise flooding loss (m^3)	Alice Kaggwa Road flooding loss (m^3)	Kamwokya Kisalosalo Road flooding loss (m^3)	Aggregate (m^3)/% of total flood loss
RE1 (52.6 mm)	149,000	64,000	78,000	291,000/57
T10 (113.7 mm)	209,000	94,000	140,000	443,000/19
T100 (156.4 mm)	252,000	115,000	176,000	543,000/20

Note. The fifth column shows the percentage of flooding in these three locations compared to the total flooding in the catchment. RE1 is the largest recorded rainfall and *T10* and *T100* are synthetic rainfalls.

Table 3 | Results from the scenario analysis including the current scenario (1), 50% blockage of sediment and solid waste at three locations (2) and 80% blockage of sediment and solid waste at three locations (3)

Rainfall	Average runoff coefficient	Surface runoff (volume, m^3)	Flooding loss (volume, m^3)	Ratio of flooding loss to surface runoff	% increase in flooding loss compared to Scenario 1
Scenario 1 – Current sediment and solid waste deposition					
RE1	0.78	1,329,000	508,000	0.38	–
T2	0.81	1,935,000	599,000	0.31	–
T10	0.84	3,153,000	1,597,000	0.51	–
T50	0.89	4,091,000	2,273,000	0.56	–
T100	0.90	4,560,000	2,674,000	0.59	–
Scenario 2 – 50 % Sediment and solid waste deposition					
RE1	0.78	1,329,000	658,000	0.50	30
T2	0.81	1,935,000	757,000	0.39	26
T10	0.84	3,153,000	1,732,000	0.55	8
T50	0.89	4,091,000	2,538,000	0.62	12
T100	0.90	4,560,000	2,951,000	0.65	10
Scenario 3 – 80 % Sediment and solid waste deposition					
RE1	0.78	1,329,000	961,000	0.72	89
T2	0.81	1,935,000	1,229,000	0.64	105
T10	0.84	3,153,000	2,309,000	0.73	45
T50	0.89	4,091,000	3,176,000	0.78	40
T100	0.90	4,560,000	3,612,000	0.79	35
Scenario 4 – "Non-failed" UDS					
RE1	0.77	1,329,000	221,000	0.17	–57
T2	0.79	1,906,000	307,000	0.16	–49
T10	0.85	3,114,000	1,013,000	0.33	–37
T50	0.88	4,045,000	1,693,000	0.42	–26
T100	0.90	4,508,000	2,059,000	0.46	–23

Note. The flooding indicators are highlighted in light grey. *RE1* is the largest recorded rainfall and *T2–T100* are synthetic rainfalls.

The study results also suggest that the most significant residual flooding would occur in the Nakamiro secondary channel, at the locations of major culvert crossings along the main Lubigi primary channel, and in the downstream nodes located after the Hoima Road crossing.

Lastly, Scenario 5, which investigated the effect of single component (culvert crossing) failure on the resulting flooding impacts, was implemented using the critical component analysis method (Johansson & Hassel 2012). In this scenario, multiple simulations were run after changing Manning's n value of each individual crossing to a value of 100. Using this approach, the number and location of individual crossings, which, when failed, would result in the most significant whole system (global) flooding impacts in the existing Lubigi UDS, were investigated. The results suggest that the single component failure of 5 culvert crossings leads to over 100% increase in the total flood volume (Figure 14). These culvert crossings with IDs C161, LU2_127, C169, LU2_31, and C170 are located at the Kalerwe-Northern Bypass crossing, the Bwaise crossing (near Christian Life International Church), the Kawaala Road crossing, and the Hoima Road crossing (Figure 15).

DISCUSSION

Extreme rainfall analysis

The tipping bucket rain gauge used in this research records point measurements, and all sub-catchments were assigned to the same rain gauge, regardless of the distance from it. However, spatial variability of rainfall is a significant source of uncertainty

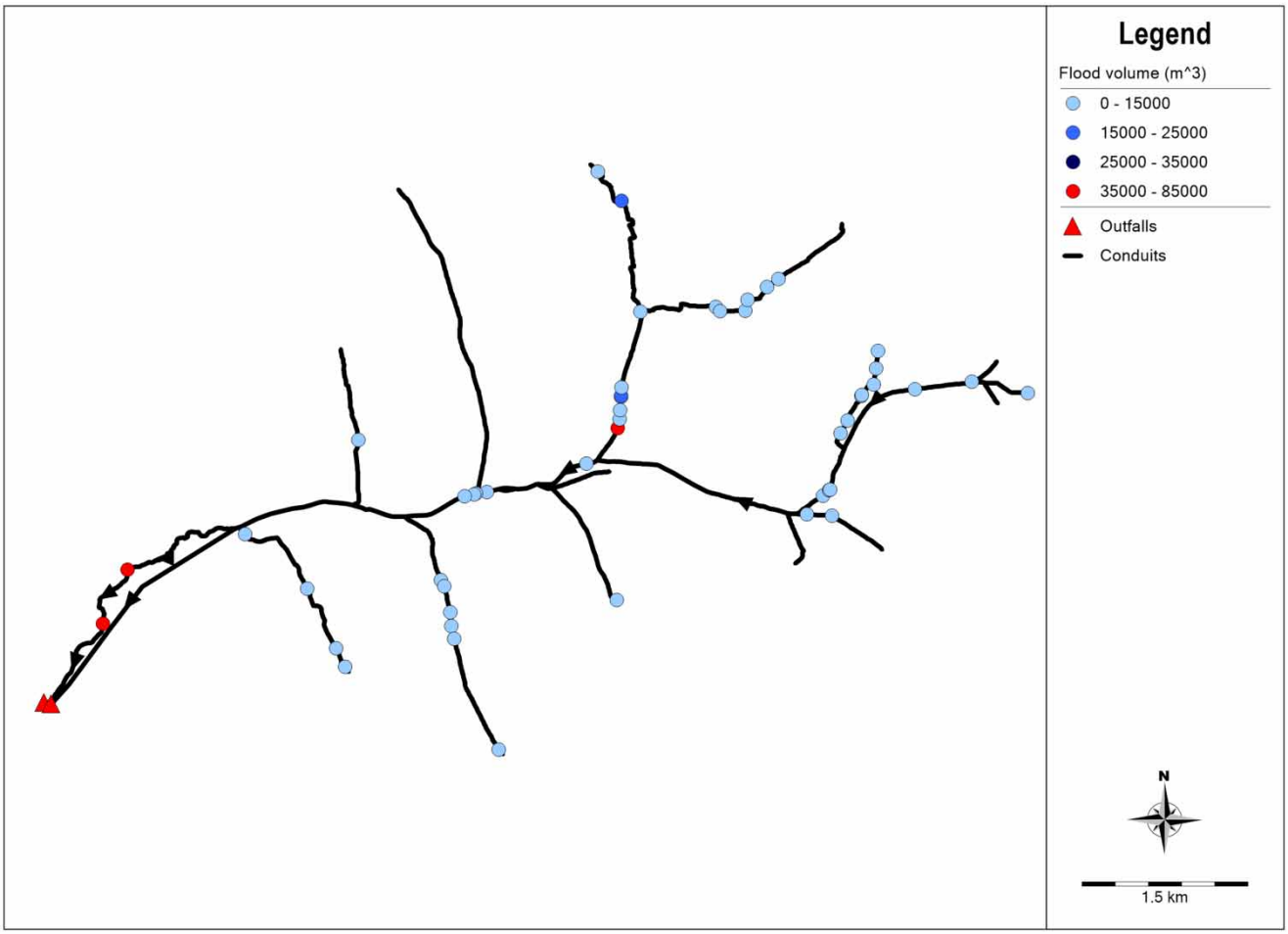

Figure 13 | 1D-model simulation results considering the 'non-failed' UDS scenario considering the observed RE1 rainfall scenario.

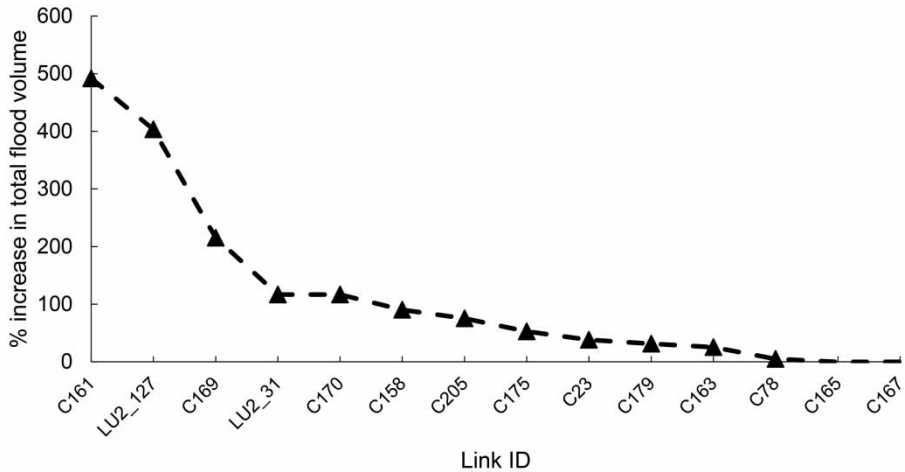

Figure 14 | Percentage increase in the total flood volume resulting from single component (culvert crossing) failures.

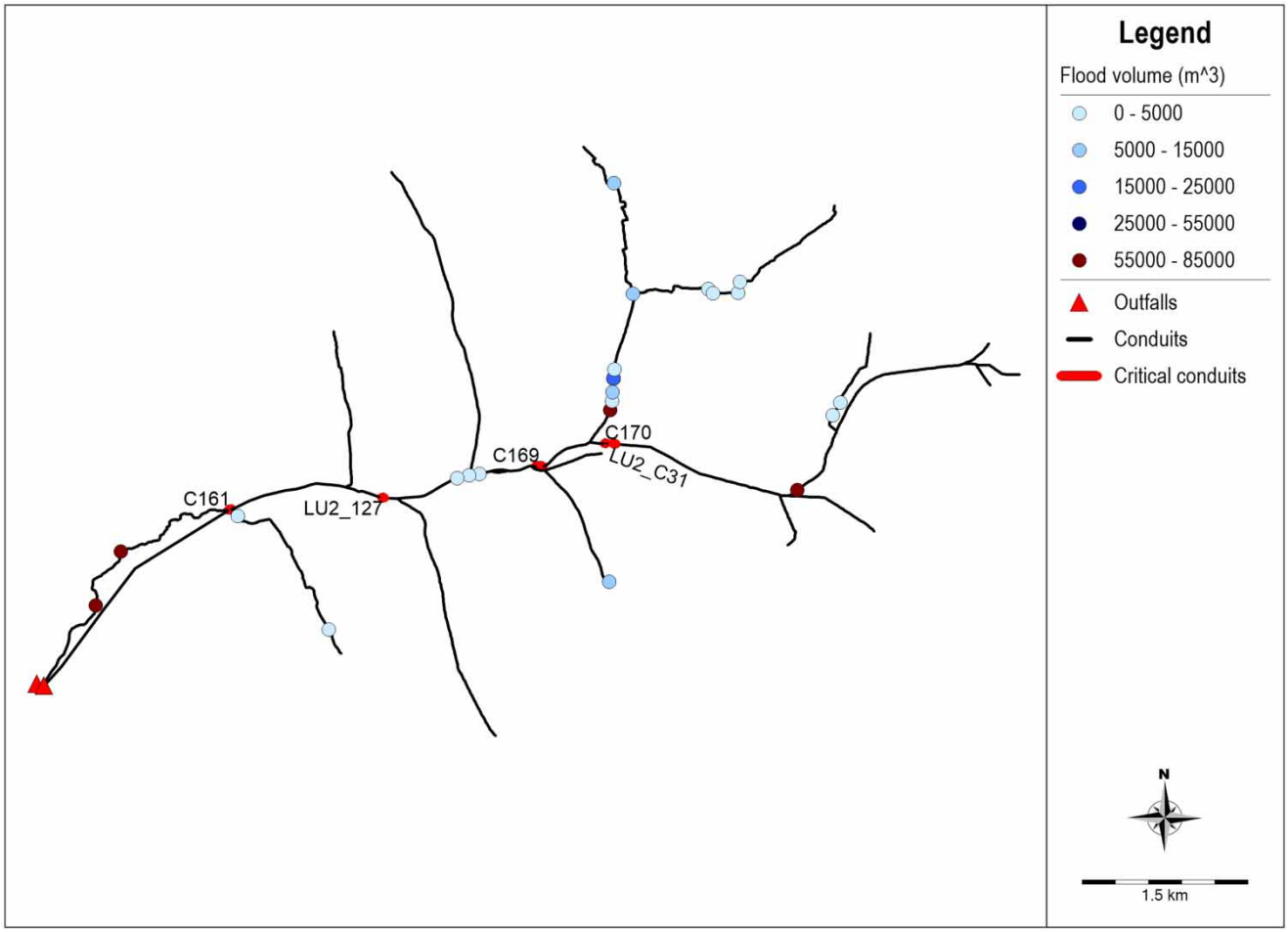

Figure 15 | Critical component analysis considering single crossing failure.

in flood modelling, regardless of the catchment size (Arnaud *et al.* 2011). In addition, the high-resolution rainfall time series collected during the study period covered a relatively short period of 2 months. Using a longer period would enhance the understanding of the temporal variability of rainfalls in Kampala and increase the likelihood of observing extreme rainfalls.

Furthermore, in a recent study based on a case study of the Nakivubo catchment in Kampala City, Mugume & Butler (2017) suggested that the use of ARFs for spatial averaging of rainfall can lead to overestimation of the magnitude of flooding resulting from spatially varied extreme rainfall events. This, therefore, underscores the need for further research focused on the derivation of area reduction factors for Kampala using relatively long high spatial and temporal resolution rainfall data collected using a dense network of automated tipping bucket rain gauges or through the use of recent gridded re-analysis satellite rainfall data products (Nakkazi *et al.* 2022; Lutz *et al.* 2024). In addition, future research could also focus on a comparative evaluation of alternative methods for creating design storms in Kampala (Guo & Zhuge 2008; Markolf *et al.* 2021).

Model performance

The model generally overestimates the observed water levels at low levels that range from 0.25 to 0.8 m and underestimates for higher water levels greater than 0.8 m (Figure 11). This discrepancy is likely due to several key limitations. First, the adopted modelling approach considered bed load sediment and solid waste deposition but did not account for the attendant transport processes. During severe flooding events, large amounts of sediment and solid waste are transported downstream through the catchment. KCCA oversees the maintenance of the UDSs in Kampala. Collecting data on the amount and frequency of the removal of deposited sediments and solid waste in the Lubigi catchment area would enhance the

understanding of sediment and solid waste transport processes, which could be used for future refinement of the developed model.

Additionally, there are uncertainties in the hydraulic data used to build the 1D model. The invert levels are based on design drawings from KCCA (2020) for a section of the primary channel, rather than as-built drawings, and the invert levels for the rest of the catchment were calculated using these invert levels along with the information from KCCA (2016). As mentioned previously, the KCCA (2016) report contains uncertainties regarding the open channels and culverts, thereby introducing uncertainty to the model.

The estimated peak water level values used in calibration and validation are uncertain as they are based on water level indications on the box culvert wall. Using this method, the time of the peak is not accurately captured. An automated water level metre would better capture the water level variations, especially when there are rapid changes after a severe storm. This enables continuous water level monitoring instead of the 2–3 daily measurements taken during the study.

In most 1D modelling studies, flood occurrence is represented using virtual cones or reservoirs on the top of each node in which floodwater is temporarily stored and allowed to flow back into the minor system when the hydraulic capacity allows (Butler *et al.* 2024). This assumption is called 'allow ponding' in PCSWMM. In this research, flooding is simulated as the water lost through overtopping of the nodes in the drainage system onto the surrounding land. The 'allow ponding' feature was tested during calibration of the model to simulate the resulting flooding impacts. However, this 1D modelling approach resulted in unreasonably high and prolonged water levels compared to the observed water levels measured at the Hoima Road box culvert crossing. On this basis, the 1D modelling option that allowed the exceedance flows to be 'lost' from the system was used to minimise the resulting errors in the simulation of water levels in the 1D minor system.

Lastly, there are uncertainties related to using a uniform PIMP value for all sub-catchments in the model. However, given that the catchment is highly urbanised, and with imperviousness levels greater than 70%, this assumption was considered plausible. Despite these uncertainties, the model validation resulted in acceptable NSE and RMSE values, indicating that the model can reliably predict real-world conditions.

Scenario analysis

The study results obtained using a calibrated and validated 1D urban drainage model have demonstrated that partial failures caused by sediment and solid waste deposition in the existing UDSs can be reliably modelled using three options. Option 1 entails the reduction of the cross-sectional areas and adjustment of the invert levels of the modelled culvert crossings (Scenarios 1, 2, and 3), Option 2 entails the adjustment of Manning's roughness coefficient for open channels and culvert crossings (Scenarios 4 and 5), while Option 3 focuses on the identification of critical culvert crossings (Scenario 5) using a critical component analysis approach (Johansson & Hassel 2012).

For Option 1, while sediment and solid waste in pipes can be straightforwardly modelled with SWMM software, there is no similar provision for modelling sediments and solid waste in open channel systems, suggesting the need to include this option in future updates of the SWMM software.

Furthermore, modelling the effect of sediment and solid waste deposition in the existing UDSs using Option 2 has been undertaken in a recent study (Mugume *et al.* 2024b). In the study, sediment and solid waste conditions were modelled using a lower bound of Manning's roughness coefficient of 0.02, representing a clean and well-maintained existing UDS ('non-failed UDS'), and an upper bound of Manning's roughness coefficient equal to 100, representing partial or full structural failure ('failed UDS') due to deposited sediment or solid waste. In Table 4, Scenario 1 in this study is compared with 'non-failed UDS' and Scenario 3 with 'failed UDS' for the Nalukolongo catchment, with similar catchment characteristics and which drains into the same receiving water body (River Mayanja) as the Lubigi catchment. In the study by Mugume *et al.* (2024b), flooding was modelled with a coupled 1D–2D model using the same IDF curves (Figure 8), but with a climate change factor of 1.2 compared to 1.3 used in this study. While this current study also included high-resolution rain data with the corresponding water level observations for calibration and validation, no such data was available for Nalukolongo.

In Table 4, a comparison between the two studies is shown. The model in this study simulates smaller flood volumes for Scenario 1 compared to the non-failed scenario in the Nalukolongo UDS, especially for smaller return periods, despite the use of larger Manning's roughness coefficients in this study. Scenario 3 shows similar flood volumes to those reported for the failed Nalukolongo UDS. However, the ratio of flooding loss to surface runoff, as highlighted in this study and presented in Table 4 indicates that the majority of runoff contributes to flooding. This could be attributed to the recent rehabilitation and expansion of Lubigi and Nakamiro drainage channels that resulted in increased hydraulic conveyance capacity in the Lubigi

Table 4 | Flood volumes from this study, compared with Mugume *et al.* (2024b), which is highlighted in light grey

Design storm	Scenario 1 Existing UDS (m^3)	Non-failed UDS (m^3)	Difference in flood volume (%)	Scenario 3 80% sediment (m^3)	Failed UDS (m^3)	Difference in flood volume (%)
T2	599,000	1,000,000	−40%	1,229,000	1,200,000	+2%
T10	1,597,000	2,100,000	−24%	2,309,000	2,500,000	−8%
T50	2,273,000	2,750,000	−17%	3,176,000	3,100,000	+2%
T100	2,674,000	3,250,000	−18%	3,612,000	3,500,000	+3%

Note.The non-failed UDS and failed UDS are based on Manning's roughness coefficients of 0.02 and 100, respectively, for all conduits.

UDS when compared to the Nalukolongo UDS which is yet to be reconstructed. As a result of this, design storms with the same characteristics result in lower flooding impacts in the Lubigi UDS (Scenario 1) when compared to the Nalukolongo UDS (Non-failed UDS Scenario).

In Option 3 (Scenario 5), critical culvert crossings, whose failure contributes to the most significant increase in flooding impacts, were identified. The results suggest that in instances of limited operation and maintenance (O&M) budgets, KCCA could focus the limited resources on targeted cleaning and maintenance of the identified critical culvert crossings and through classification and ranking of the criticality of open channel sections and pipes in the existing urban drainage network (e.g. Simone 2023).

Lastly, the study findings obtained using all the considered scenarios have demonstrated that for the modelled sediment and solid waste deposition scenarios, less water will flow through the culverts, thereby enhancing the resulting backwater effect. The study has also demonstrated that enhancing UDS asset management through improved system cleaning and maintenance initiatives (Scenario 4) results in a considerable reduction of the total flood volume resulting from the high frequency, low-magnitude rainfall events. However, the location of flooding would be shifted to more downstream areas of the catchment.

The study results also point toward the need to combine grey UDS interventions with the installation of innovative BGI options in upstream parts of the catchment, where the rainfall runoff is generated, which could delay the runoff and minimise the residual flooding that occurs during extreme events (Sörensen & Emilsson 2019; Alves *et al.* 2020; Wang *et al.* 2023; Mugume *et al.* 2024b). Additionally, restoring the natural state of the catchment by re-establishing wetlands in the highly developed upstream areas of the catchment and preventing development and informal settlements in the less developed downstream areas could further minimise future flood risk.

Locations vulnerable to flooding

Flooding is more dispersed across the catchment during long-duration rainfall, whereas shorter-duration rainfall results in more concentrated flooding at the three locations: Bwaise, Alice Kaggwa Road, and Kamwokya Kisalosalo Road. In addition, the results of the critical component analysis highlighted three additional locations, i.e. the Kalerwe-Northern bypass, Kawaala, and Hoima Road crossings, as potential flood-prone areas. The modelling study findings agree with a recent rapid flood vulnerability assessment study undertaken in Bwaise and Kalerwe zones located in the Lubigi catchment in which flood-prone areas as well as locations with flow obstructions were geo-located and mapped (Kintu 2021). The study results also agree with a recent news article published by the Uganda Radio Network, which reported an extreme flooding event that led to the loss of lives in Bwaise (Kimumbasa zone) and Kalerwe-Northern bypass (Mukwaya zone) in the Lubigi catchment (Kamali 2024).

Flooded location: Bwaise

The highest volume of flooding occurs at Bwaise (Table 2), which is located downstream in the catchment, receiving water from 4 secondary channels. One possible explanation for the extensive flooding could be a backwater effect (Cappato *et al.* 2022), caused by high flow velocities upstream of the box culvert crossing on the Nakamiro Channel (location 2, Figure 16) and the sharp angle where the secondary channel enters the main channel.

Running the model with the observed 53.4 mm rain event results in a maximum flow of 20, 16, and 25 m^3/s at locations (1), (2), and (3), respectively, (Figure 16). The small increase in flow in location (3) indicates that there could be turbulence and a loss of energy in the junction, causing the water level to rise at location (1), leading to flooding. To further analyse this,

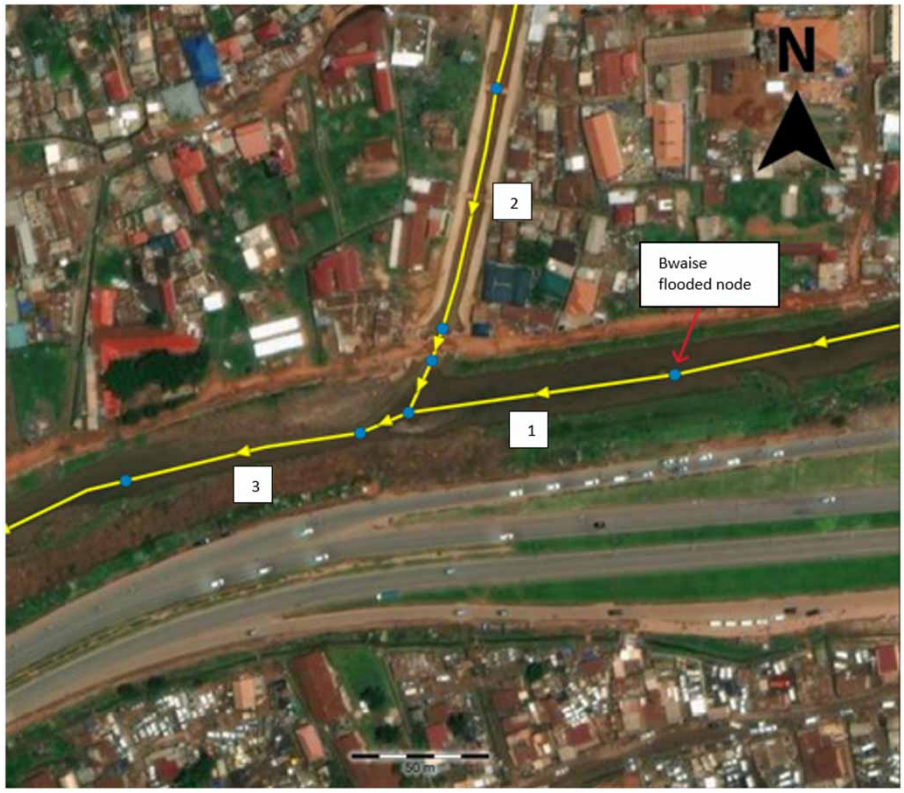

Figure 16 | Nakamiro crossing where (1) is located upstream of the crossing on the Lubigi channel, (2) is located upstream of the crossing on the Nakamiro channel, and (3) downstream of the crossing.

developing a coupled 1D–2D model would help capture the water level after flooding occurs. A 2D model – whether a standalone 2D rain-on-grid model or a coupled 1D–2D model – would also represent the flood extent and depths across the catchment area, which a 1D model alone is unable to provide. In addition, the 2D model could be used to assess the effectiveness of BGI or a flood barrier in the crossing in preventing water from flooding the surrounding areas. However, the only available digital elevation model (DEM) for this size of the catchment had a resolution of only 30 × 30 m, and there were high vertical differences compared to the invert levels of the conduits as documented by KCCA. This discrepancy poses challenges in creating accurate 2D models. Mark *et al.* (2004) recommend a 1 × 1 m–5 × 5 m resolution for urban flood modelling, as roads, sidewalks, and buildings can be captured with this level of detail. Lastly, more complex numerical modelling approaches, such as computational fluid dynamics modelling, could be applied in future research to investigate the influence of channel confluence design on flow conditions and flood risk in the existing UDSs.

Flooded locations: Alice Kaggwa Road and Kamwokya Kisalosalo Road

Alice Kaggwa Road is a culvert crossing consisting of four circular pipes with a head and wing wall at the entrance. In the field, the diameter of each pipe was approximated to be 1 m. Kamwokya Kisalosalo Road has a similar culvert design but with three pipes, instead of four. One reason for the significant flooding in both places could be undersized culvert crossings. Running the model with the rain event *RE1* results in an entrance flow of 16 and 25 m^3/s and an exit flow of 10 and 7.5 m^3/s for Alice Kaggwa and Kamwokya Kisalosalo, respectively. This indicates that both culverts act as bottlenecks, leading to flooding at the entrance of each culvert. This conclusion is strengthened by the fact that Kamwokya Kisalosalo Road has fewer pipes and is experiencing a larger volume of flooding (Table 2) along with a greater reduction in flow compared to Alice Kaggwa Road. It is noteworthy that the KCCA (2016) report describes both crossings as having box culverts. However, on-site observations confirmed they are circular culverts with smaller dimensions. Changing to box culverts with larger dimensions at both locations would potentially reduce flooding at these locations.

CONCLUSIONS AND RECOMMENDATIONS

This research has investigated the impact of sediment and solid waste deposition, combined with extreme rainfall, on urban flooding in the upper Lubigi catchment in Kampala. Using PCSWMM software, a 1D hydraulic model was developed to simulate various scenarios of sediment and solid waste deposition in combination with extreme rainfall events. The collected high-resolution rainfall data and water level observations in combination with field observations were used for model calibration and validation. This is, to the authors' knowledge, the first systematic research attempt to develop a calibrated and validated urban drainage model, considering sediment and solid waste deposition scenarios and using high-resolution rain data and the corresponding water level observations in Uganda.

The study results, obtained using a calibrated and validated 1D urban drainage model, have demonstrated that partial failures caused by sediment and solid waste deposition in the existing UDSs can be reliably modelled with three main approaches: (a) reduction of the cross-sectional areas and adjustment of the invert levels of the modelled culvert crossings, (b) adjustment of Manning's roughness coefficient for open channels and culvert crossings, and (c) use of the critical component analysis methodology. The study findings have also demonstrated that for all modelled sediment and solid waste deposition scenarios, less water will flow through the open channel and culvert cross-sections, thereby enhancing the backwater effects and increasing the risk of flooding in upstream areas.

The study has also demonstrated that enhancing UDS asset management through improved system cleaning and maintenance initiatives can result in a considerable reduction of flooding impacts caused by high-frequency and low-magnitude rainfall events. In addition, the study has underscored the need to combine grey UDS interventions with the installation of innovative BGI options to enhance the general resilience of the existing UDSs.

Based on the study findings, future research focused on (a) Improved estimation of area reduction factors and design storms in cities using relatively high-resolution rainfall and water level measurements or gridded re-analysis satellite rainfall data products, (b) More comprehensive modelling of sedimentation in open channel drainage systems through comparison of the combinations of reduced cross culvert and open channel cross-sections with the corresponding results obtained using adjustment of Manning's roughness coefficients, and (c) Modelling of multi-phase water and sediment flow conditions in open channel drainage systems using computational fluid dynamics modelling approaches, is recommended.

This research addresses a critical research gap and presents a new approach for the evaluation of the effect of scenario combinations of extreme rainfall and sediment and solid waste deposition on pluvial flood risk in data-scarce cities. The presented research can inform decision-makers in the selection and prioritisation of strategies for enhancing urban flood resilience and sustainable water management in cities.

ACKNOWLEDGEMENTS

It is given to the Directorate of Water Resources Management (DWRM), Ministry of Water and Environment, Uganda, and Kampala Capital City Authority (KCCA) for provisioning the data sets used in the study. The insights of three anonymous reviewers are also gratefully acknowledged.

FUNDING

This study was made possible through grants from Åforsk, Miljöfonden, and Sveriges Ingenjörer in Sweden and from the ARUA/U21 Early Career Researcher Collaboration Award 2023.

DATA AVAILABILITY STATEMENT

All relevant data are included in the paper or its Supplementary Information.

CONFLICT OF INTEREST

The authors declare there is no conflict.

REFERENCES

Adeke, D. P. & Mugume, S. N. (2025) A methodology for development of flood-depth-velocity damage functions for improved estimation of pluvial flood risk in cities, *Journal of Hydrology*, **653** (132736), 1–17. https://doi.org/10.1016/j.jhydrol.2025.132736.

Alves, A., Vojinovic, Z., Kapelan, Z., Sanchez, A. & Gersonius, B. (2020) Exploring trade-offs among the multiple benefits of green-blue-grey infrastructure for urban flood mitigation, *Science of The Total Environment*, **703** (134980), 1–14. https://doi.org/10.1016/j.scitotenv.2019.134980.

Arinabo, D. (2022) Unveiling the role of contextual factors in the evolution of urban floods in Sub-Saharan Africa: lessons from Kampala city, *Environmental Science & Policy*, **137**, 239–248. https://doi.org/10.1016/j.envsci.2022.09.001.

Arnaud, P., Lavabre, J., Fouchier, C., Diss, S. & Javelle, S. P. (2011) Sensitivity of hydrological models to uncertainty in rainfall input, *Hydrological Sciences Journal*, **56** (3), 397–410. https://doi.org/10.1080/02626667.2011.563742.

Balbastre-Soldevila, R., García-Bartual, R. & Andrés-Doménech, I. (2019) A comparison of design storms for urban drainage system applications, *Water*, **11** (757), 1–15. https://doi.org/10.3390/w11040757.

Barthelémy, N., Fru, F. M., Ludovic, N. J., Njila, N. & Césaire, R. (2016) Validation of models used for simulating solid domestic wastes and soil sediments flow in urban drainage systems, *International Journal of Advanced Research in Science, Engineering and Technology*, **3** (12), 3078–3083.

Butler, D., Digman, C., Makropoulos, C. & Davies, J. W. (2024) *Urban Drainage*, 5th edn. Boca Raton and Abingdon: CRC Press, Taylor and Francis Group.

Cappato, A., Baker, E. A., Reali, A., Todeschini, S. & Manenti, S. (2022) The role of modeling scheme and model input factors uncertainty in the analysis and mitigation of backwater induced urban flood-risk. *Journal of Hydrology*, **614** (128545), 1–16. https://doi.org/10.1016/j.jhydrol.2022.128545.

Chen, S. S., Kimirei, I. A., Yu, C., Shen, Q. & Gao, Q. (2022) Assessment of urban river water pollution with urbanization in east Africa, *Environmental Science and Pollution Research*, **29** (27), 40812–40825. https://doi.org/10.1007/s11356-021-18082-1.

Chitwatkulsiri, D., Miyamoto, H., Irvine, K. N., Pilailar, S. & Loc, H. H. (2022) Development and application of a real-time flood forecasting system (RTFlood system) in a tropical urban area: a case study of ramkhamhaeng polder, Bangkok, Thailand, *Water*, **14** (1641), 1–21. https://doi.org/10.3390/w14101641.

Chow, V. T., Maidment, D. R., Mays, L. W. & Chow, V. T. (1988) *Applied Hydrology*. New York: McGraw-Hill Publishing Company.

Fiddes, D., Forsgate, J. A. & Grigg, A. O. (1974) *The Prediction of Storm Rainfall in East Africa*. TRRL Laboratory Report 623, Department of the Environment, Crowthorne.

Guo, Y. & Zhuge, Z. (2008) Analytical probabilistic flood routing for urban stormwater management purposes, *Canadian Journal of Civil Engineering*, **35** (5), 487–499. https://doi.org/10.1139/L07-131.

Habonimana, H. V. (2014) *Integrated Flood Modeling In Lubigi Catchment Kampala*. Enschede: University of Twente.

Haghighatafshar, S., Becker, P., Moddemeyer, S., Persson, A., Sörensen, J., Aspegren, H. & Jönsson, K. (2020) Paradigm shift in engineering of pluvial floods: from historical recurrence intervals to risk-based design for an uncertain future, *Sustainable Cities and Society*, **61** (102317), 1–10. https://doi.org/10.1016/j.scs.2020.102317.

IPCC (2023) *Climate Change 2023: Synthesis Report. Contribution of Working Groups I, II and III to the Sixth Assessment Report of the Intergovernmental Panel on Climate Change*. In: Core Writing Team, Lee, H. & Romero, J. (eds.) Geneva: Intergovernmental Panel on Climate Change. https://doi.org/10.59327/IPCC/AR6-9789291691647.

Johansson, J., Hassel, H., (2012) Modelling, simulation and vulnerability analysis of interdependent technical infrastructures. In: Hokstad, P., Utne, I. B. & Vatn, J. (eds.) *Risk and Interdependencies in Critical Infrastructures – A Guideline for Analysis*. London: Springer, pp. 49–65.

Kamali, J. M. (2024) Residents of Kawempe Division Urge KCCA to Rehabilitate Lubigi Drainage Channel. *Uganda Radio Network*. Available at: https://ugandaradionetwork.net/story/residents-of-kawempe-division-urge-kcca-to-rehabilitate-lubigi-drainage-channel.

KCCA (2016) *Kampala Drainage Master Plan 2016: Final Technial Report*. Kampala: Kampala Capital City Authority.

KCCA (2020) *Consultancy Servicesfor Design Review of Drainage Improvement Works in Kampala: Detailed Drawings for Lot 1 – Lubigi Primary Channel and Lot 2 – Nakamiro Secondary Channel*. Kampala: Kampala Capital City Authority.

Kintu, I. M. (2021) *Community Flood Mapping Activity in Bwaise and Kalerwe, Uganda*. Youthmappers. Available at: https://www.youthmappers.org/post/2019/08/20/community-flood-mapping-activity-in-bwaise-and-kalerwe-uganda.

Kiyengo, R., Majaliwa, M., Twinomuhangi, R. & Waswa, H. (2019) Spatio-temporal flood trends & settlement choice in flood-prone areas. A case study of Lubiji micro-catchment, Kampala city, *International Journal of Environmental Studies*, **77** (3), 480–491.

Krvavica, N. & Rubinić, J. (2020) Evaluation of design storms and critical rainfall durations for flood prediction in partially urbanized catchments, *Water*, **12** (7), 1–20. https://doi.org/10.3390/w12072044.

Lutz, J., Roksvåg, T., Dyrrdal, A. V., Lussana, C. & Thorarinsdottir, T. L. (2024) Areal reduction factors from gridded data products, *Journal of Hydrology*, **635** (131177), 1–12. https://doi.org/10.1016/j.jhydrol.2024.131177.

MacAfee, E. A. & Löhr, A. J. (2024) Multi-scalar interactions between mismanaged plastic waste and urban flooding in an era of climate change and rapid urbanization, *Wiley Interdisciplinary Reviews: Water*, **11** (e1708), 1–13. https://doi.org/10.1002/wat2.1708.

Maksimović, Č., Prodanović, D., Djordjević, S., Boonya-Aroonnet, S., Leitão, J. P. & Allitt, R. (2009) Overland flow and pathway analysis for modelling of urban pluvial flooding, *Hydraulic Research*, **47** (4), 512–523. https://doi.org/10.3826/jhr.2009.3361.

Mark, O., Weesakul, S., Apirunmanekul, S., Boonya-Aroonnet, S. & Djordjeviś, S. (2004) Potentials and limitations of 1D modelling of urban flooding. *Journal of Hydrology*, 299 (3–4), 284–299. https://doi.org/10.1016/j.jhydrol.2004.08.014.

Markolf, S. A., Chester, M. V., Helmrich, A. M. & Shannon, K. (2021) Re-imagining design storm criteria for the challenges of the 21st century, *Cities*, **109** (102981), 1–11. https://doi.org/10.1016/j.cities.2020.102981.

Min, A. K. & Tashiro, T. (2024) Assessment of pluvial flood events based on monitoring and modeling of an old urban storm drainage in the city center of Yangon, Myanmar, *Natural Hazards*, **120**, 8871–8892. https://doi.org/10.1007/s11069-024-06555-8.

Møller-Jensen, L., Agergaard, J., Andreasen, M. H., Kofie, R. Y., Yiran, G. A. B. & Oteng-Ababio, M. (2023) Probing political paradox: urban expansion, floods risk vulnerability and social justice in urban Africa, *Journal of Urban Affairs*, **45** (3), 505–521. https://doi.org/10.1080/07352166.2022.2108436.

MoWT (2010) *Road Design Manual, Volume 2: Drainage Design*. (Issue January). Entebbe: Ministry of Works and Transport.

Mugume, S. N. (2015) *Modelling and Resilience-Based Evaluation of Urban Drainage and Flood Management Systems for Future Cities*. Exeter: University of Exeter. Available at: https://ore.exeter.ac.uk/repository/handle/10871/18870.

Mugume, S. N. & Butler, D. (2017) Evaluation of functional resilience in urban drainage and flood management systems using a global analysis approach, *Urban Water Journal*, **14** (7), 727–736. https://doi.org/10.1080/1573062X.2016.1253754.

Mugume, S. N. & Nakyanzi, L. P. (2024) Evaluation of effectiveness of blue-green infrastructure for reduction of pluvial flooding under climate change and internal system failure conditions, *Blue-Green Systems*, **6** (2), 264–292. https://doi.org/10.2166/bgs.2024.030.

Mugume, S. N., Gomez, D. E., Fu, G., Farmani, R. & Butler, D. (2015) A global analysis approach for investigating structural resilience in urban drainage systems, *Water Research*, **81**, 15–26. https://doi.org/10.1016/j.watres.2015.05.030.

Mugume, S. N., Abasabyoona, G., Engwau, J., Sempewo, J. I., Van de Sande, B. & Butler, D. (2024a) Assessing the impact of the rise in lake Victoria water levels on urban flooding using a GIS-based spatial flood modelling approach, *Urban Water Journal*, **21** (2), 219–233. https://doi.org/10.1080/1573062X.2023.2284960.

Mugume, S. N., Kibibi, H., Sorensen, J. & Butler, D. (2024b) Can blue-green infrastructure enhance resilience in urban drainage systems during failure conditions?, *Water Science and Technology*, **89** (4), 915–944. https://doi.org/10.2166/wst.2024.032.

Nakkazi, M. T., Sempewo, J. I., Tumutungire, M. D. & Byakatonda, J. (2022) Performance evaluation of CFSR, MERRA-2 and TRMM3B42 data sets in simulating river discharge of data-scarce tropical catchments: a case study of Manafwa, Uganda, *Journal of Water and Climate Change*, **13** (2), 522–541. https://doi.org/10.2166/wcc.2021.174.

Nimusiima, A., Faridah, N., Isaac, M., Bob, A. O. & Peter, W. (2021) A community perspective of flood occurrence and weather forecasting over Kampala city, *African Journal of Environmental Science and Technology*, **15** (5), 188–201. https://doi.org/10.5897/ajest2021.3007.

OECD/UN/ECA/AfDB (2022) *Africa's Urbanisation Dynamics 2022: the Economic Power of Africa's Cities*. Paris: OECD Publishing. https://doi.org/10.1787/3834ed5b-en.

Olsson, H. (2024) *Modellingthe Effect of Sediment and Solid Waste Deposition on Urban Flooding in Kampala, Uganda*. Division of Water Resources Engineering, Department of Building and Environmental Technology, Lund University, Lund. Available at: https://lup.lub.lu.se/student-papers/record/9169315/file/9169331.pdf.

Ortega Sandoval, A. D., Sörensen, J., Rodríguez, J. P. & Bharati, L. (2023) Hydrologic–hydraulic assessment of SUDS control capacity using different modeling approaches: a case study in Bogotá, Colombia, *Water Science & Technology*, **87** (12), 3124–3145. https://doi.org/10.2166/wst.2023.173.

Owusu, G. & Oteng-Ababio, M. (2015) Moving unruly contemporary urbanism toward sustainable urban development in Ghana by 2030, *American Behavioral Scientist*, **59** (3), 311–327. https://doi.org/10.1177/0002764214550302.

Pérez-Molina, E., Sliuzas, R., Flacke, J. & Jetten, V. (2017) Developing a cellular automata model of urban growth to inform spatial policy for flood mitigation: a case study in Kampala, Uganda, *Computers, Environment and Urban Systems*, **65**, 53–65. https://doi.org/10.1016/j.compenvurbsys.2017.04.013.

Pervin, I. A., Rahman, S. M. M., Nepal, M., Haque, A. K. E., Karim, H. & Dhakal, G. (2020) Adapting to urban flooding: a case of two cities in south Asia, *Water Policy*, **22**, 162–188. https://doi.org/10.2166/wp.2019.174.

Quang, C. N., Giang, N. N., Hoa, H. V. & Hung, P. Q. (2022) Effects of sediment deposit on the hydraulic performance of the urban stormwater drainage system, *IOP Conference Series: Earth and Environmental Science*, **964** (012020), 1–7. https://doi.org/10.1088/1755-1315/964/1/012020.

Richmond, A., Myers, I. & Namuli, H. (2018) Urban informality and vulnerability: a case study in Kampala, Uganda, *Urban Science*, **2** (22), 1–13. https://doi.org/10.3390/urbansci2010022.

Ritter, A. & Muñoz-Carpena, R. (2013) Performance evaluation of hydrological models: Statistical significance for reducing subjectivity in goodness-of-fit assessments. *Journal of Hydrology*, **480**, 33–45. https://doi.org/10.1016/j.jhydrol.2012.12.004.

Rossman, L. & Simon, M. A. (2022) *Storm Water Management Model (SWMM) User's Manual Version 5.2*. Cincinnati: US Environmental Protection Agency.

Simone, A. (2023) Vulnerability assessment of urban drainage network using relevance-based centrality metrics, *River*, **2** (1), 39–51. https://doi.org/10.1002/rvr2.30.

Sliuzas, R., Jetten, V., Flacke, J., Lwasa, S., Wasige, J. & Pettersen, G. (2013) *Flood Risk Assessment, Strategies and Actions for Improving Flood Risk Management in Kampala*. (Issue November). University of Twente, Faculty of Geo-Information Science and Earth Observation (ITC), Enschede.

Sohn, W., Kim, J. H., Li, M. H., Brown, R. D. & Jaber, F. H. (2020) How does increasing impervious surfaces affect urban flooding in response to climate variability?, *Ecological Indicators*, **118** (106774), 1–12. https://doi.org/10.1016/j.ecolind.2020.106774.

Sörensen, J. & Emilsson, T. (2019) Evaluating flood risk reduction by urban blue-green infrastructure using insurance data, *Journal of Water Resources Planning and Management*, **145** (2), 1–11. https://doi.org/10.1061/(asce)wr.1943-5452.0001037.

Trisos, C. H., Adelekan, I. O., Totin, E., Ayanlade, A., Efitre, J., Gemeda, A., Kalaba, K., Lennard, C., Masao, C., Mgaya, Y., Ngaruiya, G., Olago, D., Simpson, N. P., Zakieldeen, S., (2022) Africa: climate change 2022: impacts, adaptation and vulnerability. In: Pörtner, K. M. H.-O., Roberts, D. C., Tignor, M. & Poloczanska, E. S. (eds.) *Climate Change 2022: Impacts, Adaptation and Vulnerability*. Cambridge and New York: IPCC, pp. 1285–1455. https://doi.org/10.1017/9781009325844.011.1286.

Wang, M., Liu, M., Zhang, D., Zhang, Y., Su, J. & Zhou, S. (2023) Assessing hydrological performance for optimized integrated grey-green infrastructure in response to climate change based on shared socio-economic pathways, *Sustainable Cities and Society*, **91** (104436), 1–14. https://doi.org/10.1016/j.scs.2023.104436.

Wu, J., Ma, Y. & Song, S. (2024) Reducing particle accumulation in sewers for mitigation of combined sewer overflow impacts on urban rivers: a critical review of particles in sewer sediments, *Water Science and Technology*, **89** (1), 89–115. https://doi.org/10.2166/wst.2023.394.

First received 17 December 2024; accepted in revised form 28 February 2025. Available online 10 March 2025